Iacomino *et al. Biochar* (2024) 6:82
https://doi.org/10.1007/s42773-024-00378-3

Biochar

ORIGINAL RESEARCH Open Access

Biochar aging, soil microbiota and chemistry of charcoal kilns in Mediterranean forests

Giuseppina Iacomino[1], Mohamed Idbella[2*], Luigi di Costanzo[1], Giandomenico Amoroso[1], Emilia Allevato[1], Ahmed M. Abd-ElGawad[3] and Giuliano Bonanomi[1,4]

Abstract

Charcoal kilns, old structures used for charcoal production in the forest, preserve a charcoal-enriched topsoil representing a suitable proxy for studying the long-term effect of biochar addition to soil. Two kiln platforms located at Gelbison and Vesole mountain sites in Southern Italy were selected due to their comparable climates but distinct parent rocks. We conducted standard soil chemical analyses and used next-generation sequencing to explore bacterial and fungal microbiome. Anthracology identified charcoal species, while scanning electron microscopy (SEM) with energy dispersive X-ray spectroscopy (EDS) characterized charcoal particles. Reflectance Fourier transform infrared spectroscopy (DRIFTS) assessed biochar surface oxidation. Additionally, a bioassay with soybean, maize, and Tomato investigated the impact of kiln soil on plant performance. Our results showed that kiln soils did not exhibit higher pH, cation exchange capacity, or greater richness in cations. EDS and FTIR analyses showed that charcoal buried in forest soil for decades undergoes significant oxidation, with increased O/C ratio and the presence of oxygenated functional groups. Charcoal surfaces were selectively enriched with Ca^{2+} on limestone substrate sites but with Al and Si over sedimentary (flysch) substrate. While differences in the kiln soil and its surroundings were noticeable, they were not drastic in terms of microbial diversity and composition. Surprisingly, the bioassay indicated that the kiln microbiota had a more positive impact on plant growth compared to external forest soil. In conclusion, this study highlights the unique nature of kiln microsites and begins to unveil the enduring effects of charcoal accumulation on soil chemistry and microbiota in forest soil.

Highlights

- Kiln soils did not exhibit higher pH, cation exchange capacity, or greater richness in cations.
- Charcoal in forest kilns underwent significant oxidation with increased O/C ratio and presence of oxygenated functional groups.
- Charcoal surface showed different enrichment of Ca, Al, and Si influenced by the parent rock.
- Kiln microbiota exhibited a positive influence on plant growth, hinting at ecological benefits.

Keywords Anthracology, Charcoal kilns, Biochar, Soil chemistry, *Terra Preta*, Microbiome

*Correspondence:
Mohamed Idbella
mohamed.idbella@um6p.ma; mohamed.idbella@unina.it
Full list of author information is available at the end of the article

Graphical Abstract

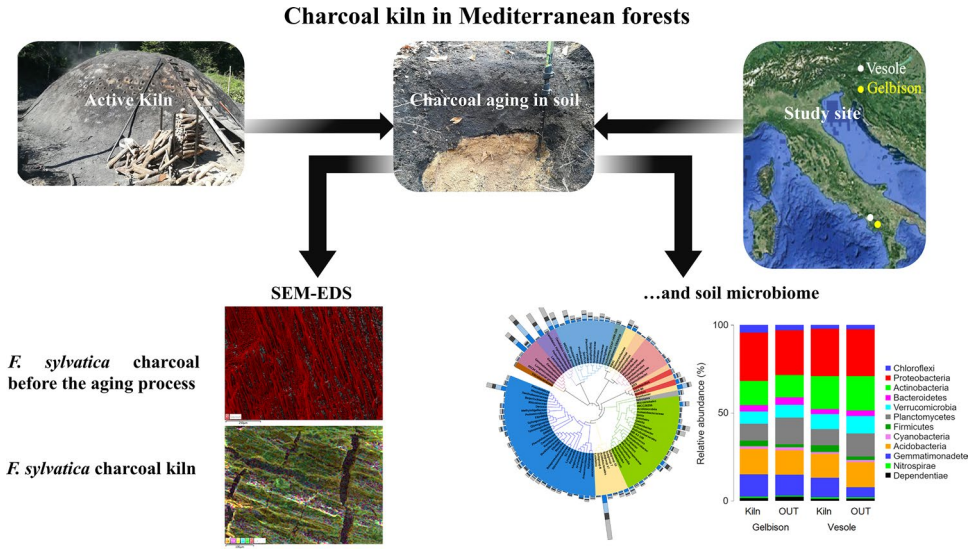

1 Introduction

Throughout human exploitation of the mountain environment, charcoal kilns (or hearths) have played a significant role as operational platforms for the production of charcoal (Snitker et al. 2022). These characteristic bases are present in many archaeological sites and are widespread in anthropogenic forest landscapes in different geographical areas including USA (Straka 2014), Central and Southern America (Seligson et al. 2017), Northern Europe (Deforce et al. 2021), and Mediterranean basin (Carrari et al. 2017). Although charcoal platforms have a long history of use, they have been largely overlooked for several decades in various regions, including Italy. However, a handful of sites still remain active, particularly in remote areas of the Apennines.

Anthropogenic charcoal kiln production introduces enduring topographic and pedological features into the forest landscape. Charcoal kilns could become a pervasive feature of the landscape, reaching a density higher than 1 per ha, influenced by factors such as forest productivity and proximity to metal mines and furnaces (Garbarino et al. 2022). Ecological consequences of charcoal kilns, and the study of these structures, have undergone an intensification in the last decade. Due to the stratification of charcoal remains, studies on kilns represent a valuable source of information for the reconstruction of past vegetation through charcoal analysis as well as the radiocarbon dating method (Knapp et al. 2013). Notably, the analysis of sixteen charcoal kilns of the Bavarian Forest (Germany) aimed to understand woodland composition and its landscape changes within the last 500 years (Nelle 2003). Residual accumulation of charcoal can be quantitatively very high and surpass 30% of the soil volume, especially in the upper section of the soil profile (Wiedner et al. 2015; Fouché et al. 2023). The presence of a high amount of pyrogenic organic carbon has important implications for the structure and function of these soils. The discovery of "*terra preta*" or "dark earth", created by pre-Columbian people of Amazonia forests (Glaser 2007), has sparked intense research into the possible exogenous applications of biochar in agroecosystems (Lehmann and Joseph 2015).

The accumulation of carbon in the soil has significant functional implications due to the physical and chemical characteristics of this material. Biochar is the material produced by pyrolysis, a process occurring at temperatures ranging from 200 to > 900 °C under limited oxygen availability. Wood biochar is typically characterized by a high C/N ratio and very high content of organic carbon that confers resistance to microbial degradation. In agricultural context, biochar added to soil has a liming effect (Bolan et al. 2023), but also increases water retention capacity (Novak et al. 2013), as well as the ability to adsorb putative phytotoxic organic molecules (Oleszczuk et al. 2012) and increases cation exchange capacity (Dey et al. 2023). In Wallonia, Belgium, the soil within charcoal kiln has larger C/N ratio and cation exchange capacity but was depleted in exchangeable K^+ and available P compared to adjacent soil (Hardy et al. 2016). Bayuzick et al. (2023) found in Appalachian, USA that kiln soil has

unique patterns of chemistry being richer, compared to control soil, of total organic carbon, Mg^{2+} and Ca^{2+}. In the Apennines, Carrari et al. (2016) found that soil under kiln platform has higher total organic carbon, total N, and higher pH compared to control soil. Interestingly, that author also reported that kiln platforms represented a hostile microsite for the recolonization of deciduous and evergreen woody species.

The estimated average residence time of wood biochar varies from centuries to millennia (Lehmann and Joseph 2015). The long-term impact of natural forces such as precipitation, oxidation, temperature variation, and biodegradation on biochar is termed aging (Liu and Chen 2022). This process can induce changes in the physicochemical properties of biochar, including its elemental composition, specific surface area (SSA), surface morphology, pH, and ion exchange capacity (Wang et al. 2020a, b), consequently affecting its performance over time. A significant portion of studies on biochar aging have utilized artificially accelerated aging methods, such as drying or wetting and chemical oxidants (Sultana et al. 2011; Cross and Sohi 2013). Other approaches involve promoting aging through the activity of microorganisms, which can be enhanced by supplementing labile organic compounds like glucose or fresh biomass (Keith et al. 2011). Generally, as biochar undergoes progressive aging, it tends to reduce in size, and surface functional groups such as carboxyl, carbonyl, or hydroxyl are formed. Consequently, aged biochar has the potential to enhance interactions with soil organic matter, soil minerals, nutrients, and contaminants (Mia et al. 2017). Moreover, the physical properties of biochar, particularly SSA and pore volume, can vary depending on the extent of aging or chemical oxidation, thus influencing its sorption capacities (Rajapaksha et al. 2016). Therefore, the application of aged biochar holds promise as a tool for enhancing agricultural productivity while concurrently contributing to climate change mitigation.

Several studies relying on kiln sites in Northern Europe and the Apennines assessed the long-term effects of biochar on soil chemical properties. While many reports investigated the short-term effect of exogenously applied biochar on microbiome including beneficial microbes (Wu et al. 2022; Idbella et al. 2024), and plant pathogens (Iacomino et al. 2022), there has been less studies on the long-term effect of kiln on soil microbiome composition, structure, and diversity using next-generation sequencing (Bayuzick et al. 2023). For example, Lasota el al. (2021) found that fungal and bacterial diversity, as well as species and genera richness, were higher at charcoal hearth sites compared to non-charcoal-enriched sites, despite the otherwise similar habitat types. Indeed, utilizing such historical sites could enhance our understanding of the long-term effects of biochar on soil chemical and biological properties for better application across different environmental contexts. Therefore, in this study, we aimed to describe the soil of charcoal kiln platforms and its microbiota composition as compared with that of the surrounding soil. We employed a combination of soil chemistry analyses and the next-generation sequencing techniques to determine how the soil microbiota is shaped by kiln platform microsite. Additionally, we assessed charcoal ageing inside kilns by scanning electron microscopy and energy dispersive spectroscopy (SEM–EDS). Finally, given the lack of long-term field experiments with biochar, we sought to utilize the kiln site as natural models to investigate long-term effects. For this reason, we carried out a bioassay with three crops, soybean (*Glycine max*), corn (*Zea mays*), and tomato (*Solanum lycopersicum*), to explore the potential impact of soil kiln containing fragmented and aged biochar on plant performance. Based on current knowledge, the specific hypotheses tested in this study were as follows:

i. The soils of charcoal kilns have higher pH, cation exchange capacity, and are richer in organic carbon, as well as key nutrients such as N, P, K^+, Ca^{2+}, and Mg^{2+};
ii. the long-term natural oxidation of coal leads to significant changes both in the surface morphology and in the elemental composition, reflecting the mineral nature of the soil of origin;
iii. The soils of charcoal pits harbor a more diverse microbiome, both in terms of bacteria and fungi;
iv. Crop growth is anticipated to be greater in soils enriched with charcoal from kilns.

2 Material & methods

2.1 Study sites

The present study was carried out in two sites positioned in the National Park of Cilento e Vallo di Diano, Southern Italy: Mont Vesole (40°24′33.92"N, 15°09′19.47"E; 1197 m a.s.l.) and Mont Gelbison (40°12′15.79"N, 15°20′51.27"E; 1270 m a.s.l.) (Fig. 1). Vegetation in both sites was closed, monospecific forest stand dominated by European beech, i.e., *Fagus sylvatica* (average height of the trees was 22 and 27 m at Vesole and Gelbison study sites, respectively). The two sites share a similar mountain Mediterranean climate with cool, wet winter and relatively warm and dry summer season. Climatic time series recorded at the closest meteorological station from the study sites, located at Capaccio at 419 m a.s.l. (6 km from Vesole and 28 km from Gelbison) showed mean annual precipitations of 1128 mm, monthly temperatures ranging between maxima of 23 °C (August) and 6 °C

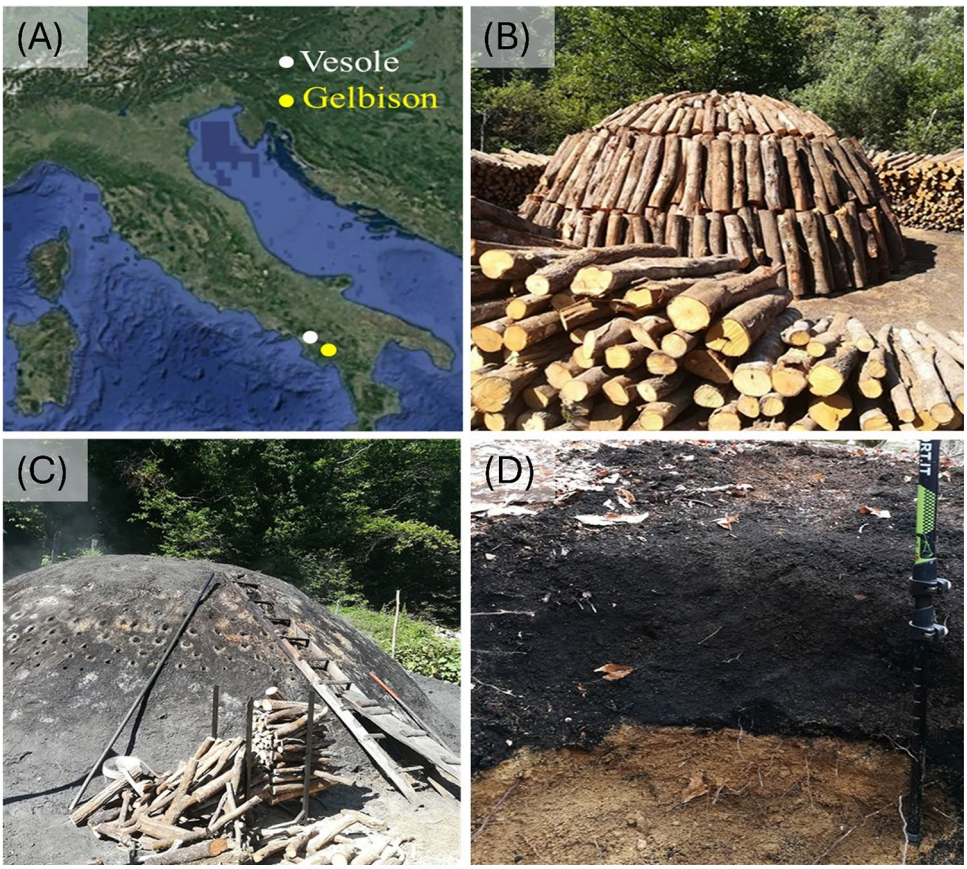

Fig. 1 Geographical location of the two study sites in Southern Italy **A** Pictures of a charcoal kiln outside the sampling points starting operations **B** and during the pyrolysis process **C**. Pictures B and C are reported as illustrative examples of historical charcoal production processes and were taken in 2022 in Calabria about 150 km from the study site. Soil profile (**D**) in a kiln area on Mount Gelbison, note the black charcoal-rich layer (about 30 cm thick) above the yellow sandstone soil. Pictures by Giuliano Bonanomi

(January) with a mean annual temperature of 15.1 °C. The mean annual temperature at the study sites has been calculated using a 0.006 °C m^{-1} adiabatic lapse rate of temperature change with elevation on data retrieved from WorldClim 2.0 (http://www.worldclim.org; Hijmans and Jarvis 2005) at a spatial scale resolution of 1 km^2. Based on these calculations, the mean annual temperature was 10.5 °C at Vesole and 10.2 °C at Gelbson. The main difference between the two sites is the geomorphological feature, with sedimentary (flysch) overlying clay soils in Gelbison and limestone rocks with abundant rock outcrops at Vesole (ISPRA 2023). On the slopes of Mount Gelbson, medium-deep soils are found with thick superficial horizons on a marly-arenaceous substrate, with a fine texture and good oxygen availability, classifiable as Haplic Umbrisols. Differently, on the slopes of the limestone mountains like Vesole, steep soils are found to have medium depth, with the presence of deposits of volcanic ash with a medium texture and good oxygen availability, classifiable as Molli-Vitric Andosols (Di Gennaro 2002).

At both study sites, the kiln platform microsites were easily recognizable due to their flat terrace-like shape and the dark color of the soil determined by the accumulation of charcoal residues. These charcoal kiln sites, rich in centuries-old charcoal remains due to their resistance to microbial decomposition, represent the legacies of wood charcoal production endured for centuries in Europe (Nocentini et al. 2013). They were probably abandoned after World War II mainly due to changed socio-economic conditions. Indeed, while wood charcoal production experienced a decline in northern and central Europe during the nineteenth century with the widespread adoption of coal, its significance in the Mediterranean region actually grew during the industrial revolution due to the scarcity of alternative fuel sources (Deforce et al., 2013). Especially in Italy, production and usage markedly decreased in the 1950s (Landi and Piussi 1988).

2.2 Soil sampling and chemical analyses

During spring 2023, soil samples were collected outside (indicated as outside) and inside (indicated as kiln) platforms. Soil sampling involved utilizing a 10 cm diameter soil corer to extract samples from depths of 0–40 cm, following the removal of above-ground litter. This process was conducted at five designated points within each replicate plot, culminating in the creation of a representative composite sample per replicate. A total of three replicate samples were obtained from areas both inside the kiln platform and within a distance of 2–3 m from it. Thus, at each of the two geographically studied sites, 3 kiln replicates were randomly selected and a total of 12 samples (2 sites × 2 sampling areas (inside kiln and outside) × 3 replicates) were obtained. All samples (~ 1 kg each) were collected from the topsoil (0–40 cm), which represents the soil layer where charcoal fragment accumulate (Fig. 1). For soil chemical characterization, a total of 17 parameters were measured: pH, electrical conductivity, coarse sand, fine sand, silt, clay, total limestone, active limestone, organic carbon, total N, C/N ratio, phosphate (P), cation exchange capacity (CEC), exchangeable Ca^{2+}, exchangeable Mg^{2+}, exchangeable Na^{+} and exchangeable K^{+}. Soil chemical properties were determined on soil air-dried at 25 °C until constant weight was reached and sieved through 2 mm mesh. Electrical conductivity (EC) and pH were measured in 1:5 and 1:2.5 soil:water suspensions, respectively. Titration with chromic acid was used to measure organic C content (Walkley and Black 1934). Phosphate was measured by bicarbonate extraction (Schoenau and O'halloran 2008) using 1 g of soil samples mixed with 20 ml of 0.5 M $NaHCO_3$ (Olsen P) solution at a ratio of 1:20 (w/v). Following extraction, the samples were centrifuged at 1300 × g for 10 min, filtered, and subjected to photometric analysis at 712 nm using a Cary 60 UV–Vis spectrophotometer (Agilent Technologies). Total soil N was determined by flash combustion of 5 mg samples using an N elemental analyzer (Flash EA2000 ThermoFisher). Cation exchange capacity was measured after soil treatment with a barium chloride and triethanolamine solution at pH 8.2 back-titration with HCl (Sumner and Miller 1996). Exchangeable bases and their respective counter ions (Ca^{2+}, Mg^{2+}, K^{+}, Na^{+}) were assayed by flame atomic absorption spectrometry.

2.3 Anthracological analysis

To quantify the charcoal content present in both the kiln and outside soils, we used ~ 1 kg of soil from each of the three kiln replicates previously sampled from Vesole and Gelbison mountains, after conducting chemical and microbiological analyses. Each kiln replicate soil was air-dried and subsequently immersed in 2500 ml of water for 24 h to allow the charcoal particles to float. Thereafter, charcoal particles with a diameter > 2 mm were separated using a 2 mm mesh sieve. The charcoal fragments were air dried at 60 °C in an oven for 72 h, and finally weighed. This method allows a rapid estimate of the charcoal content but underestimates the total content by not including particles with a diameter smaller than 2 mm.

Subsequently, charcoal fragments were submitted to anthracological analyses for taxa identification. For each kiln, we extracted a variable number of charcoal fragments (10–20 pieces of at least 1 cm). For microscopic identification, we split charcoal samples to obtain fresh fracture planes oriented along the transverse, longitudinal radial, and longitudinal tangential directions. We used an incident light microscope Optika B-510 MET with magnifications between 50 and 500X to observe each sample and taxonomically identify the most accurate possible taxon with published references (Schweingruber 1990). We did not perform charcoal radiocarbon dating since the method is not precise for samples more recent than the industrial revolution due to the Suess effect (Keeling 1979). Finally, the charcoal elemental C, N and H contents of the samples (20 mg) were measured using an element analyzer (CHNS, Fison Instruments EA).

2.4 Charcoal aging assessed by scanning electron microscopy and energy dispersive spectroscopy (SEM–EDS)

To assess chemical changes in charcoal particles, we applied scanning electron microscopy and energy dispersive spectroscopy (SEM–EDS) with infrared spectroscopy on old charcoal fragments collected in kilns located in Vesole and Gelbson mountains. As control, we used a freshly produced *F. sylvatica* charcoal fragments. Briefly, a wood sample was pyrolyzed following an approach similar to the traditional charcoal production method used in old times in the Apennines (Fig. 1). This sample, indicated as "recent charcoal", is expected to represent *F. sylvatica* charcoal before the process of ageing that occurs when buried in the soil profile.

Both old and recent samples (dimension ~ 1 × 0.5 × 0.3 cm) were mounted on SEM stubs with a conductive carbon paint double adhesive. In order to topographically map chemical elements present in these charcoals, SEM imaging was performed with a joint probing for energy-dispersive X-ray spectroscopy (EDS). The EDS consists of a focused beam of accelerated electrons to scan and create fluorescence emissions from present elements. The energy of the emitted X-rays is characteristic for the specific atom that is excited by the primary beam and provides information about the content present in the outermost hundreds of nm to ~ 2 µm of the oven-dried sample. Field Emission Scanning Electron

Microscope (SEM) images were collected at DiSTAR—Dipartimento di Scienze della Terra, dell'Ambiente e delle Risorse—University of Napoli Federico II using a Zeiss Merlin VP Compact scanning electron microscope (SEM) coupled with an Oxford Instruments Microanalysis Unit equipped with an INCA X-act detector for EDS at room temperature. For these measurements, a working distance of 6 mm and an acceleration voltage of 15 kV beam were used. Although most of the samples were conductive and images were clear including mapping of chemical elements, fewer required sputtering coating with gold nanoparticles to obtain high-resolution images. Images with various magnifications ranging from 100 to 10,000X were obtained. SEM images were analyzed using the standard software package AZtecCrystal, which allows for the processing of data collected using electron backscatter diffraction (EBSD) (Wilkinson and Britton, 2012). Infrared spectroscopy was applied to old samples from Vesole and Gelbson as well as to recent F. sylvatica charcoal. Briefly, dried charcoal particles were ground using a mortar and pestle, followed by analysis through diffuse reflectance infrared Fourier-transform spectroscopy (DRIFT) and recorded with a PE Spectrum-One spectrometer equipped with a diffuse reflectance accessory, and by accumulating up to 100 scans with a resolution of 4 cm^{-1}. DRIFT, known for its applicability to highly scattering and absorbing materials, was employed to measure the diffuse reflection of infrared radiation from the samples, providing insights into the functional groups present on the charcoal surface. FTIR measurements were recorded from 7 mm pellets obtained by homogeneously mixing 2 mg of biochar material and dried KBr. The normal frequency range of absorption observed for our samples has been compared with those of standard functional groups reported in literature (Silverstein et al. 2015). Radiation spectra were recorded in the range of 4000–500 cm^{-1}, with a potassium bromide pellet as a reference. Absorption spectra were subsequently derived from the recorded radiation spectra. To optimize data quality, the spectra were confined to a range of 3750–700 cm^{-1}, eliminating any unusable portions. A baseline correction, specifically the concave rubber band correction, was applied to enhance the accuracy of the results.

2.5 Soil microbiome: DNA extraction, amplification, sequencing and data analyses

The extraction of DNA from terra preta soils can pose challenges due to reduced DNA extraction efficiencies and PCR amplification rates (Jin 2010). Such discrepancies stemming from biochar presence could yield misleading results when molecular methods are employed to analyze microbial communities. Several mechanisms have been proposed to explain the decreased efficiency of DNA extraction in the presence of biochar. These include biochar's surface cation exchange properties, which may lead to DNA adsorption through cation-bridging interactions with the negatively charged phosphate backbone of DNA (Pietramellara et al. 2009). Additionally, biochar's known effects on pH have been shown to influence DNA sorption to soil surfaces (Chan et al. 2008). Moreover, components of soil organic matter can contaminate extracted DNA with PCR-based downstream applications inhibitors (Watson and Blackwell 2000). If biochar adsorbs or releases components similar to these humic compounds, they could interfere with extraction reagents or copurify with DNA. Furthermore, biochar provides additional protective pore spaces and enhances aggregate stability, potentially shielding cells from complete lysis during DNA extraction (Kimetu and Lehmann 2010). In a previous study, Leite et al. (2014) compared DNA extraction methodologies for biochar-amended soils using commercial kits and found the PowerSoil protocol to be the most effective. For this reason, our DNA extraction was carried out from 0.5 g of soil, sub-collected after mixing well the 1 kg soil samples from each kiln replicate and then stored at − 80 °C, using the DNeasy PowerSoil Kit (QIAGEN, USA) following the manufacturer's guidelines. Following extraction, we assessed DNA concentration and purity using a Nanodrop 2000 (ThermoFisher, USA) and verified its integrity via agarose gel electrophoresis. For high-throughput sequencing targeting bacteria and fungi, we focused on amplifying the V3/V4 regions of the 16S rRNA gene (approximately 460 bp) and the ITS1-2 subunits of the internal transcribed spacers (about 300 bp). PCR amplification was performed using the primers S-D-Bact-0341-b-S-17/S-D-Bact-0785-a-A-21 (Berni Canani et al. 2017) and BITS1fw/B58S3-ITS2rev (Bokulich and Mills 2013), following the respective conditions as indicated in the original studies. The PCR products were purified using Agencourt AMPure beads (Beckman Coulter, Milan, IT) and quantified using an AF2200 Plate Reader (Eppendorf, Milan, IT). Equimolar pools were prepared, and sequencing was performed on an Illumina MiSeq platform, generating paired-end reads of 2 × 250 bp.

Demultiplexed fastq files underwent a series of data processing steps to generate unique amplicon sequence variants (ASVs) following the DADA2 pipeline (Callahan et al. 2016). Briefly, the raw sequences were trimmed to a length of 250 base pairs, with primer sequences removed. Subsequently, filtering criteria included maxN = 0, maxEE = 2, and truncQ = 2. Error rates were estimated via the learnErrors function, utilizing nearly 4 million reads. The data algorithm was employed for de-replication and precise identification of sequence

variants, followed by the removal of chimeras using the RemoveBimeraDenovo function. For the fungal pipeline, using Cutadapt software (Martin 2011), an initial step encompassed adapter and low-quality end trimming. Taxonomic assignments were performed using the SILVA and UNITE databases for bacteria and fungi, respectively (Quast et al. 2013; Nilsson et al. 2019). To refine the dataset, *Chloroplast* and *Streptophyta* contaminants were eliminated, and singleton ASVs were removed, followed by recalculating the relative abundance.

Alpha diversity metrics, specifically the number of reads and Shannon index, were computed using PRIMER 7 software (Primer-E Ltd., Plymouth, UK). Boxplots representing these metrics were generated using the ggplot2 package within RStudio version 4.2.2. For assessing community composition at the lowest taxonomic levels, heatmaps were constructed. These heatplots were utilized to cluster variables based on an index of association similarity and to cluster samples according to Bray–Curtis dissimilarity. The heatplots display the 60 most abundant taxa within the fungal and bacterial communities. To investigate the influence of charcoal within kilns on microbial phylogeny, maximum likelihood phylogenetic trees were constructed for the top 100 frequently detected ASVs using MEGA-X. These trees were visualized and interactively explored using the Interactive Tree of Life (iTOL v6, http://itol.embl.de). Moreover, to explore the differential abundance of taxa between soil samples from kilns and outside kilns, the Statistical Analysis of Metagenomic Profiles (STAMP) software package (ver. 2.0.9) was employed. Significance testing was carried out using Mann–Whitney and Kruskal–Wallis H tests. Statistically significant characteristics were further investigated using post hoc tests (Tukey–Kramer) to identify specific groups within the profiles that exhibited differences from each other.

2.6 Plant bioassay

To investigate the impact of charcoal on the soils of temperate forests, a greenhouse experiment was conducted from March to August 2023 using three target species: *Glycine max*, *Zea mays*, and *Solanum lycopersicum*. These species were chosen due to their short lifespan, being agricultural annuals, and their classification into different functional types, specifically a nitrogen-fixing species, a grass, and an herb, respectively.

The plants were cultivated in pots (19 cm of opening diameter ∗ 17 cm of height ∗ 14 cm of base diameter) filled with soils previously collected. In each pot, five seeds were sown, and two plants were kept in each pot upon germination. Seeds underwent surface sterilization in a 3% sodium hypochlorite solution for 1 min and were thoroughly rinsed with sterile water before use. This experiment consisted of five replicates for each of the three plant species, grown in two soil types: soil collected from Gelbison or Vesole mountains. Additionally, the plants were subjected to two treatments: one inside kilns and the other outside kilns, and two types of soil conditions: sterilized and non-sterilized, resulting in a total of 120 pots. Before the start of the experiment, the soil was sterilized through autoclaving at 1 atm pressure and 120 °C for one hour, repeated 3 times with a 24-h interval. The pots were housed in a greenhouse (minimum/maximum/average temperature, 12.5/30.4/22.7 °C; relative humidity, 40/88/69%) within the Department of Agriculture (Federico II University of Naples, Italy), and regularly watered to maintain field capacity. No mineral fertilizers were added to the soils. Pots were arranged in a randomized block design, and to prevent potential contamination between pots, either through leaching or splashing during watering, each pot was placed inside an individual plastic pot saucer. After 4 months, plants were harvested, and the shoots were clipped at soil surface, dried at 70 °C in a ventilated chamber for 3 days, and their dry weights were recorded. Data collected from the pot experiments were subjected to a factorial analysis of variance (ANOVA) to discern the primary and interactive impacts of the fixed factors, which included target plants, parent rock type, kiln status, and sterilization status. To compare individual means, post hoc Tukey's pairwise comparisons test was employed. Significance levels were determined at a threshold of $P < 0.05$. All statistical analyses were conducted using STATISTICA 13.3 software. Furthermore, the impact of soil sterilization on plant shoot biomass was evaluated through the application of the Relative Sterilization Index (RSI; Bonanomi et al. 2021b, a), derived from the Relative Interaction Index (RII) introduced by Armas et al. (2004). For each target species, the RSI was calculated as follows:

$$RSI = (SB_S - SB_{NS})/(SB_S + SB_{NS})$$

where SB_S represents the shoot biomass measured in sterile soil, while SB_{NS} denotes the corresponding value in non-sterile soil. The index ranges from +1 to −1, with positive values indicating increased shoot biomass in sterile soil conditions and negative values indicating enhanced biomass in non-sterile soil conditions.

3 Results

3.1 Chemical soil properties

The pH was not statistically different while the electrical conductivity was higher for outside soil compared to the kiln in both study sites (Table 1). The soil texture was not different between kiln and outside with the exception of the clay fraction which was slightly higher in the outside soil. According to parent rock

Table 1 Physical and chemical parameters of soil collected inside kiln and outside at Gelbison and Vesole mountains

	Unit	Gelbison		Vesole	
		Kiln	Outside	Kiln	Outside
pH		6.11 ± 0.3a	5.96 ± 0.2a	6.83 ± 0.2 a	6.93 ± 0.3 a
Electrical conductivity	mS m^{-1}	2.72 ± 0.2 b	5.46 ± 0.5 a	4.47 ± 0.4 b	18.21 ± 1.2 a
Coarse sand	g Kg^{-1}	496 ± 32 a	529 ± 43 a	424 ± 26 a	272 ± 27 b
Thin sand	g Kg^{-1}	393 ± 12 a	312 ± 21 a	412 ± 34 a	454 ± 33 a
Silt	g Kg^{-1}	93 ± 8 a	97 ± 11 a	137 ± 12 a	159 ± 21 a
Clay	g Kg^{-1}	18 ± 2 b	62 ± 8 a	27 ± 3 b	115 ± 11 a
Total limestone	g Kg^{-1}	2.91 ± 0.2 a	0.00 b	3.50 ± 0.4 a	3.43 ± 0.3 a
Active limestone	g Kg^{-1}	2.47 ± 0.3 a	0.00 b	16.04 ± 3 b	27.3 ± 5 a
Organic carbon	g Kg^{-1}	37.73 ± 3 a	30.42 ± 2 b	53.77 ± 7 b	96.32 ± 8 a
Total nitrogen	g Kg^{-1}	2.46 ± 0.1 a	1.89 ± 0.1 b	4.18 ± 0.3 b	8.38 ± 0.7 a
C/N ratio		15.36 ± 1.4 a	16.11 ± 1.5 a	12.82 ± 1.1 a	11.54 ± 0.9 a
Assimilable phosphorus	mg Kg^{-1}	14.33 ± 2.4 a	12.81 ± 2.1 a	18.52 ± 1.8 b	28.01 ± 1.5 a
Cation exchange capacity (CEC)	meq 100 g^{-1}	20.31 ± 2.1 a	18.32 ± 1.9 a	45.44 ± 4.2 b	67.17 ± 5.1 a
Exchangeable Ca^{2+}	meq 100 g^{-1}	1.70 ± 0.7 a	2.54 ± 0.9 a	23.73 ± 1.5 b	60.62 ± 4.3 a
Exchangeable Mg^{2+}	meq 100 g^{-1}	0.31 ± 0.2 a	0.54 ± 0.4 a	1.46 ± 0.9 a	4.47 ± 1.0 b
Exchangeable Na^{+}	meq 100 g^{-1}	0.02 ± 0.001 a	0.01 ± 0.001 a	0.23 ± 0.005 a	0.27 ± 0.004 a
Exchangeable K^{+}	meq 100 g^{-1}	0.16 ± 0.07 a	0.17 ± 0.05 a	0.86 ± 0.1 b	1.52 ± 0.2 a

Vales are average ± standard deviation, different letters indicate statistically significant differences between kiln and outside soils (Paired T test, $P < 0.05$)

type, total limestone but most of all active limestone they were higher at the Vesole, characterized by a calcareous substrate, than at the Gelbison. At Vesole site the active limestone was higher for outside soil than kiln. The organic carbon content and total nitrogen in Gelbison was higher in the kiln than outside, whereas in Vesole it was significantly higher in the outside than in the kiln. At Gelbison the CEC, P, K^{+}, Ca^{2+}, Mg^{2+} and Na^{+} content was not different between kiln and outside. Differently, at Vesole CEC, P, K^{+}, Ca^{2+}, Mg^{2+} and Na^{+} contents were higher in the outside than in the kiln. Elemental analysis revealed that the recent charcoal exhibited the highest carbon content (80.56%) among the three, accompanied by moderate N content (0.86%) and a relatively low hydrogen content (2.36%). This resulted in a C/N ratio of 93.67, indicative of its composition. Conversely, Vesole displayed lower carbon content (59.43%) but a slightly higher N content (0.44%) compared to Gelbison. However, Vesole showed the highest hydrogen content (3.51%) among the three samples, leading to a C/N ratio of 135.07. This discrepancy underscores distinct compositional variations among the samples. Gelbison, on the other hand, showed the lowest N content (0.31%) but a relatively high carbon content (65.51%). Its hydrogen content (2.68%) fell between recent charcoal and Vesole. Notably, Gelbison exhibited the highest C/N ratio of 218.33, suggesting distinct characteristics compared to the other samples (Table 2).

Table 2 Elemental composition analysis of Recent charcoal, Vesole, and Gelbison samples including percentages of Nitrogen (N), Carbon (C), and Hydrogen (H), and C/N and O/C ratio

Sample	N (%)	C (%)	H (%)	C/N	O/C
Recent charcoal	0.86 ± 0.04 a	80.56 ± 2 a	2.36 ± 0.8 b	93.67 c	0.06 c
Vesole	0.44 ± 0.03 b	59.43 ± 5 b	3.51 ± 0.7 b	135.07 b	0.41 b
Gelbison	0.30 ± 0.08 b	65.51 ± 4 b	2.68 ± 0.6 ab	218.33 a	0.81 a

Vales are average ± standard deviation, different letter indicate statistically significant differences

3.2 SEM–EDS characterization of chemical analyses

To compare differences between kilns and recent charcoal, SEM images and EDS analysis were employed to acquire the topological and elemental composition of the surface of natural charcoal particles. In Fig. 2, we compare SEM images and EDS spectra of recent and old samples from Gelbison and Vesole kilns. As anticipated, the recent charcoal from *F. sylvatica* exhibits primarily carbon. In contrast, the elemental mapping of kiln charcoals indicates a heterogeneous presence of silicate mixtures containing Al and Ca (Fig. 2, Figure S1 a, b). In addition, the presence of some composite material and iron can be revealed. Moreover, the samples show a well-organized and characteristic porous morphology resembling a vegetable plant-cell pattern of *F. sylvatica* (Fig. 2). Marked differences can be noticed from comparison of SEM images and EDS spectra between Gelbison

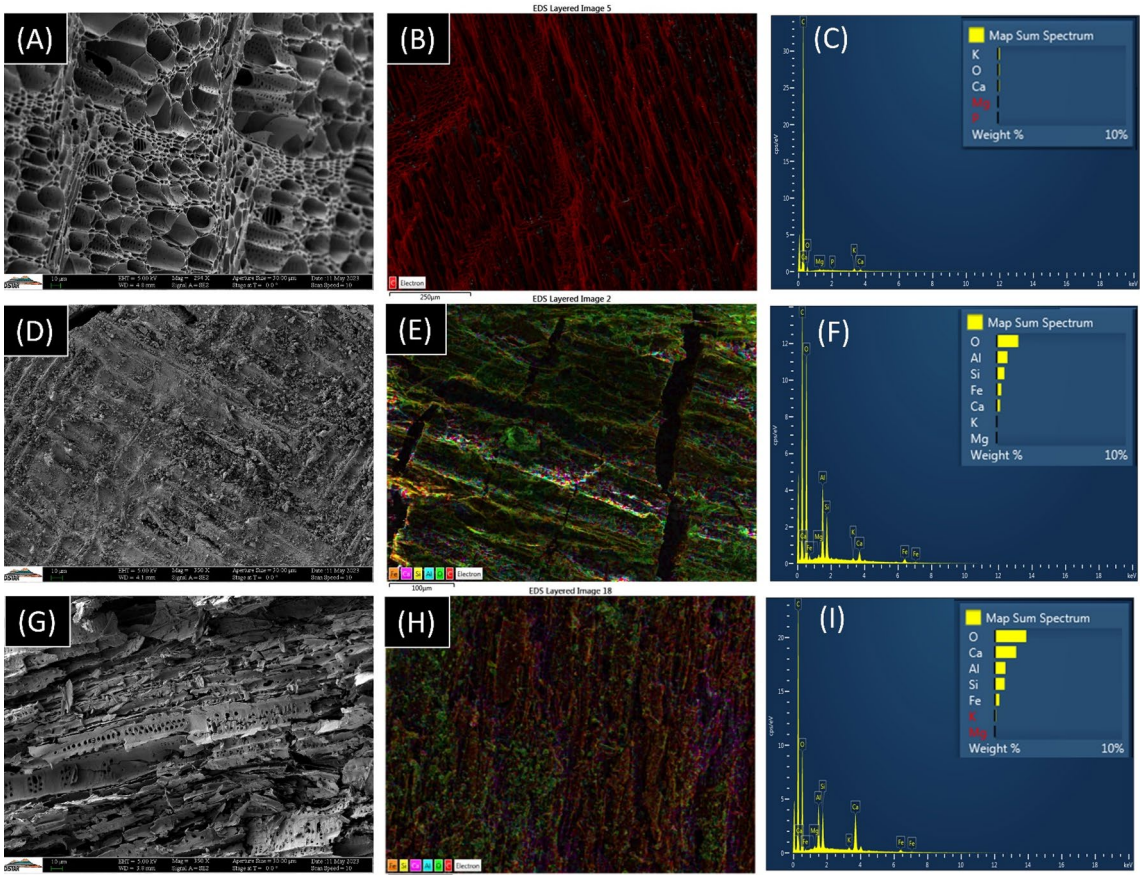

Fig. 2 Scanning electron micrograph (SEM) of recent collected charcoal from *Fagus sylvatica* **a** charcoal collected from kiln at Gelbison **d** and charcoal collected from kiln at Vesole **g** (scale bar, 250 µm). The colour map shows the heterogeneous elemental distribution of C, Ca, O, Al, Si, P, and K in (**b**, **e**, **h**) (scale bar, 100 µm). The corresponding X-ray energy dispersive spectra (EDS) of the regions, are shown in the right column (**c**, **f**, **i**)

and Vesole kilns (Fig. 2d–i). Gelbison charcoal shows the presence of a strong O signal in addition to C, Si, and Al. The signal ratio of these elements suggests the presence of mixtures of Al silicate (Figure S1a). Differently, Vesole charcoal shows the presence of a strong C signal and combined with its ratio to O and Ca suggests presence of limestone (Figure S1b). The presence of limestone is agreement with the parent rock present in its native soil. Traces amount of iron are also present. The chemical analyses support the presence in Vesole charcoal of a higher amount of organic coating also supported by SEM and EDS analysis (Table 1, and Figure S1b). The stoichiometric ratio between O and C (O/C) calculated on the basis of the SEM–EDS spectra data revealed that this was much lower for the recent charcoal (O/C = 0.06) compared to the charcoal from kiln of Gelbison (O/C = 0.81) and Vesole (O/C = 0.41) (Table 2).

3.3 Fourier transform infrared spectroscopy (FTIR)

Changes in kiln charcoal surface functionalities compared to the *F. sylvatica* recent charcoal are illustrated in Fig. 3. The FTIR spectra of Vesole and Gelbison kiln charcoal samples show a broad peak between 3567 and 3045 cm^{-1}, corresponding to O–H stretching of phenolic and alcoholic –OH, indicating a clear oxidation phenomenon. Conversely, *F. sylvatica* recent charcoal shows only a small peak at 3045 cm^{-1}. The peaks at 1612 cm^{-1} exhibit different intensities and represent –C=C– stretching of aromatic groups or carbonyl bonds (C=O) of the carboxylic groups or conjugated ketone. The C–O–C symmetric stretching in aliphatic groups and acid derivatives is evident in samples from Vesole and less in Gelbison, visible at ~ 1000 cm^{-1} (Fig. 3).

3.4 Anthracological analysis

The charcoal particles amount (particles with diameter > 2 mm) was higher in the kiln soils as charcoal was absent in the outside soils at both study sites. In detail, at Vesole the charcoal particles amount was 112.82 g kg^{-1}, while at Gelbison the amount was 157.91 g kg^{-1}. The anthracological analysis conducted on 50 charcoal pieces from Mount Vesole revealed that they exclusively belong

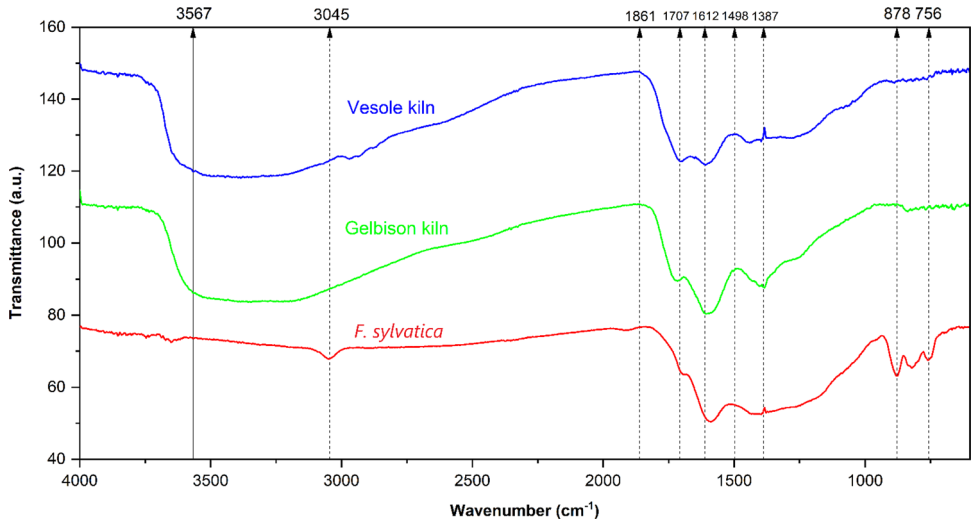

Fig. 3 Fourier-transform infrared spectroscopy (FTIR) analysis of charcoal samples collected at Vesole and Gelbison mountains, alongside the *Fagus sylvatica* recent charcoal

to *F. sylvatica* (Figure S2). For Mount Gelbison, out of 98 charcoals analyzed, 82 (83.67%) were identified as *F. sylvatica*, while 16 (16.32%) were attributed to *Ilex aquifolium*.

3.5 Plant growth

The shoot biomass of *G. max*, *Z. mays*, and *S. lycopersicum* displayed statistically significant responses based on both the plant species and soil type (Fig. 4). Specifically, the shoot biomass of *S. lycopersicum* was higher when cultivated with outside soil from Gelbison. Conversely, no statistically significant differences were observed in the shoot biomass of *Z. mays* across all soil types. For *G. max* shoot biomass was higher for the outside soil of Gelbison compared to outside Vesole.

The impact of soil sterilization varied depending on the target species and soil type (Fig. 4). In detail, the RSI index was negative for *S. lycopersicum* in all soil with the exception of outside at Vesole. For *Z. mays* RSI was lowest for kiln soil at Gelbson and highest for Vesole outside. A similar trend was found for *G. max* where the RSI was lowest for kiln soil at Gelbison and highest for outside soil of Vesole.

3.6 Soil microbiota

Significant variation in Shannon diversity and the number of ASVs was observed for both bacterial and fungal communities. The bacterial Shannon index was significantly higher in the outside soil compared to kiln in Vesole, while no statistical differences were observed for Gelbison, either for the number of bacterial ASVs or Shannon diversity index (Fig. 5B). Conversely, no statistical differences were observed regarding the fungal Shannon index and the number of ASVs between inside and outside kilns in both mountain locations (Fig. 6B).

At the phylum level, considerable and statistically significant variation was observed among soils in both the bacterial and fungal communities. All the soils under examination predominantly hosted *Proteobacteria*, with percentages ranging from 25.92% outside the kiln in the Gelbison to 27.65% inside the kiln of the same mountain (Fig. 5A). In contrast, *Acidobacteria and Actinobacteria* emerged as the second most dominant phyla across all soils. Specifically, these two phyla exhibited parity inside and outside the kiln in the Gelbison. However, in the Vesole *Actinobacteria* exceeded *Acidobacteria* constituting 18.71% inside the kiln compared to 13.08% of *Acidobacteria*, and 18.43% outside the kiln compared to 14.92% of *Acidobacteri*a. Additionally, *Planctomycetes* displayed higher proportions outside the kilns in both sites, at 15.38% in Gelbison and 13.34% in Vesole, as opposed to inside the kilns, where they accounted for 9.71% in Gelbison and 8.90% in Vesole. Conversely, Gemmatimonadetes exhibited their lowest presence outside the kilns in Vesole, representing 5.85%, while they ranged between 11.77% outside the kilns in Gelbison and 12.68% inside the kilns in Gelbison for the other soil samples.

Concerning fungi, all the soils examined were predominantly characterized by the phylum *Ascomycota* with abundances ranging from 73.14% outside in Vesole to 83.16% in kilns (Fig. 6A). The highest proportion of the phylum *Basidiomycota* was identified outside the kilns in Vesole, accounting for 24.16%, followed by 21.53% inside the kilns in Gelbison, 22.19% outside in the same site,

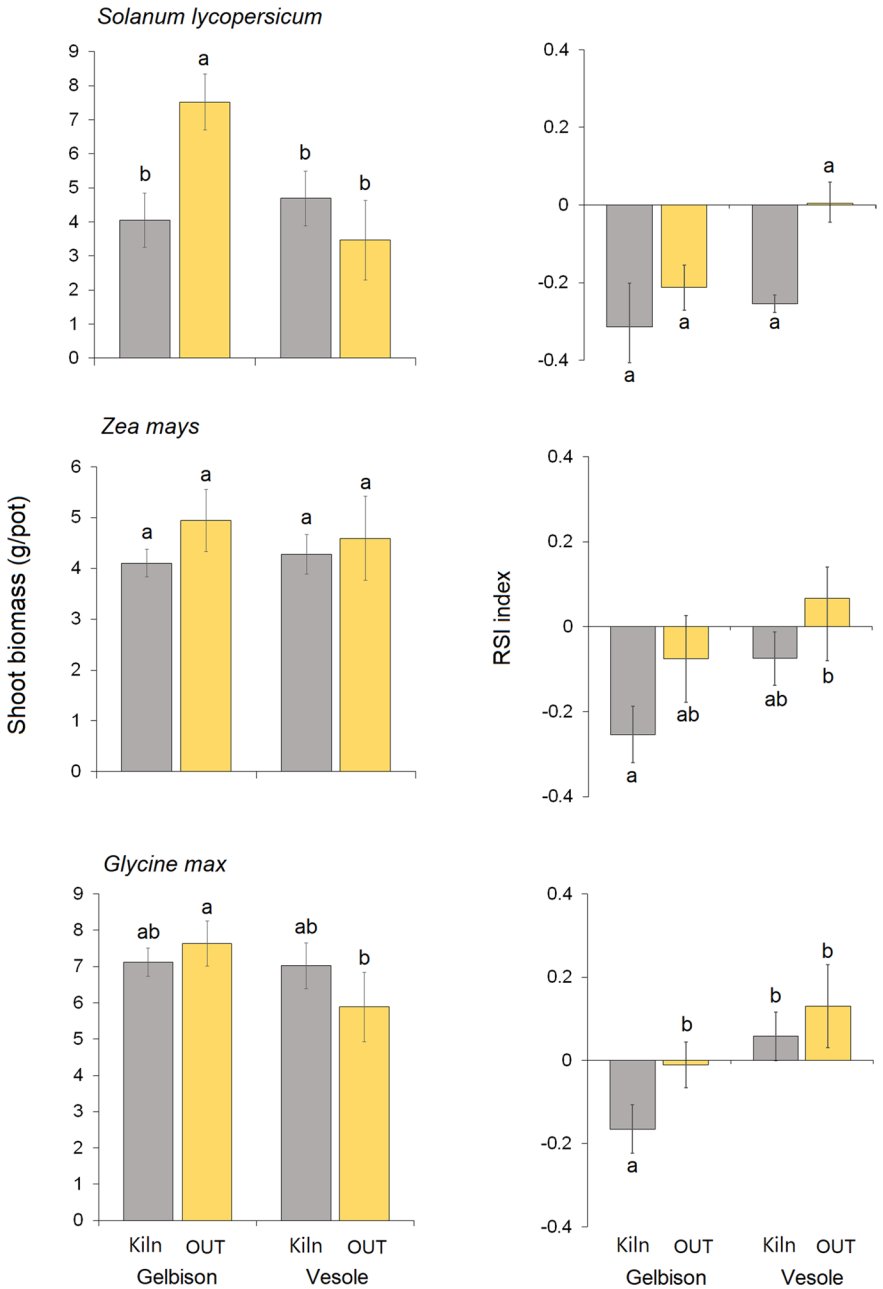

Fig. 4 Average of shoot biomass (g plant^{-1}) and the relative sterilization indices (RSI) for shoot biomass of *Glycine max*, *Zea mays*, and *Solanum lycopersicum* grown in soils collected from kiln and outside on Gelbison and Vesole mountains. RSI range is from + 1 to − 1: positive and negative mean values indicate a higher plant growth in non-sterile or sterile conditions, respectively. The error bars represent the standard deviation. Bars topped by the same letter do not differ significantly by Duncan test

while the lowest was recorded inside the kilns in Vesole, representing 13.87%. *Chytridiomycota*, on the other hand, were more abundant in kilns in both sites compared to the outside, whereas *Mortierellomycota* exhibited higher levels outside than in kilns.

At the lowest taxonomic level, as based on the 60 most frequent bacterial ASVs, the heatmap revealed a higher abundance of *Gemmatimonadaceae* for kilns of both sites in comparison to the outside (Fig. 5D). Furthermore, *Gaiella* exhibited significantly higher abundance in Vesole compared to Gelbison, whereas *Bryobacter* displayed greater abundance in Gelbison, and *Planctomycetales* were more prevalent outside the kilns of Gelbison in contrast to other soil samples. Notably,

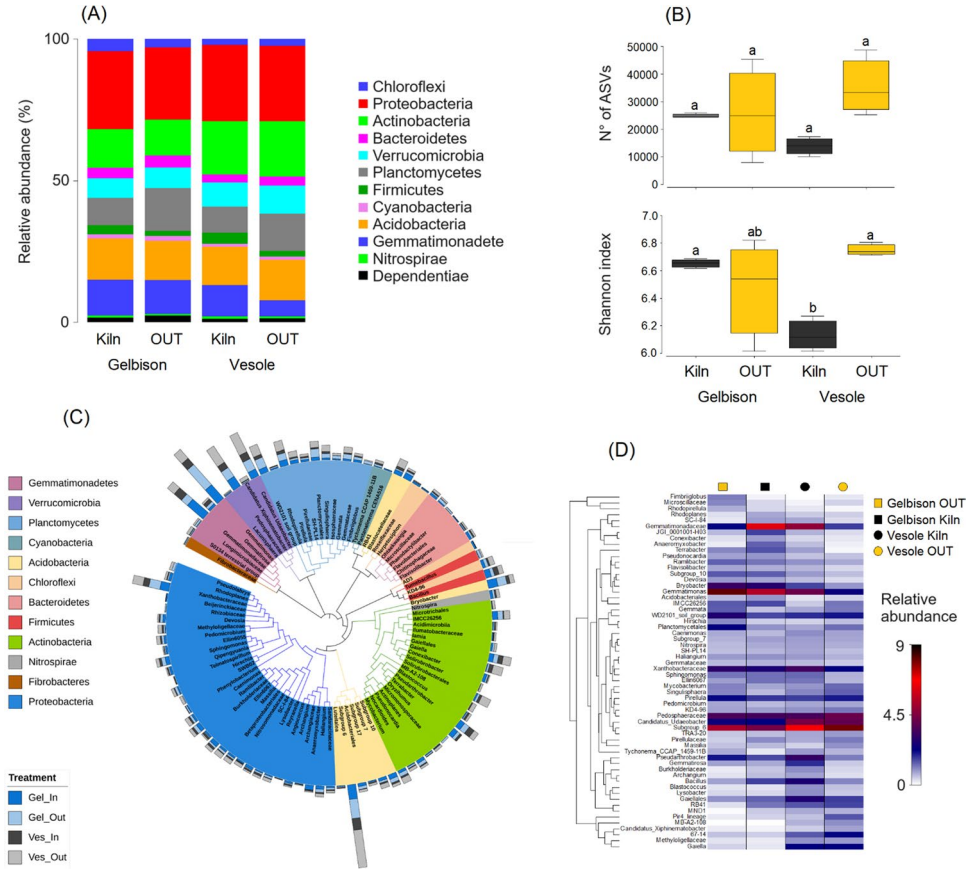

Fig. 5 **A** The relative abundance of bacterial phyla inside and outside charcoal kilns on both Gelbison and Vesole mounts. **B** Box plots show the variation in the numbers of ASVs and Shannon diversity index for bacterial communities inside and outside charcoal kilns on both Gelbison and Vesole mounts. Different letters indicate significant differences ($P < 0.05$) in the indices. **C** Phylogenetic tree displays the top 100 ASVs with the highest relative abundance. **D** Heatmap displays the relative abundance of the 60 most frequent Amplicon Sequence Variants in the bacterial communities inside and outside charcoal kilns on both Gelbison and Vesole mounts. The hierarchical clustering of variables is based on Whittaker's association index

Pedosphaeraceae, *Candidatus udaeobacter*, *Acidobacteria subgroup 6*, and *Xanthobacteraceae* displayed notably high abundance across all soils. On the other hand, concerning fungal communities, the heatmap highlighted clear variations among the tested soils, with a higher abundance of *Talaromyces* and *Coprinopsis* inside the kilns of Gelbison when compared to outside soil (Fig. 6D). Conversely, *Humicola* was more prevalent in Gelbison than in Vesole. *Agaricomycetes* and *Fusarium* were consistently present in high abundance across all soils, while *Chaetomium* was notably absent inside the kilns of Gelbison when contrasted with its high abundance in other soil samples.

In order to assess the bacterial phylogenetic diversity inside and outside the kilns of Gelbison and Vesole at a higher resolution, we used the top 100 abundant ASV sequences to taxonomically classify 16S genes from our samples (Fig. 5C). We observed that the highest ASVs, in terms of relative sequence abundance, were broadly distributed across the phylogenetic tree. In total, we identified 12 phyla among the 100 highest ASVs, with *Proteobacteria* and *Actinobacteria* dominating. Most of the dominant taxa showed equal abundance in samples collected both inside and outside the kilns in both mountains. However, *Acidobacteria subgroup 6*, *Candidatus udaeobacter*, and *Pedosphaeraceae* were more abundant outside in Vesole, while *Gemmatimonas* were more abundant outside in Gelbison. On the other hand, the fungal phylogenetic tree revealed 4 phyla among the 100 highest abundant ASVs, with *Ascomycota* dominating (Fig. 6C). Most of the identified taxa exhibited equal abundance among samples, such as *Trichoderma* and *Agaricomycetes*. *Ramaria amyloidea* was exclusively found outside the kilns in Vesole, whereas *Talaromyces veerkampii*, *Coprinopsis scobicola*, and *Gibberella baccata* were exclusively present inside the kilns in Gelbison. *Humicola grisea* showed high abundance outside the kilns in Gelbison.

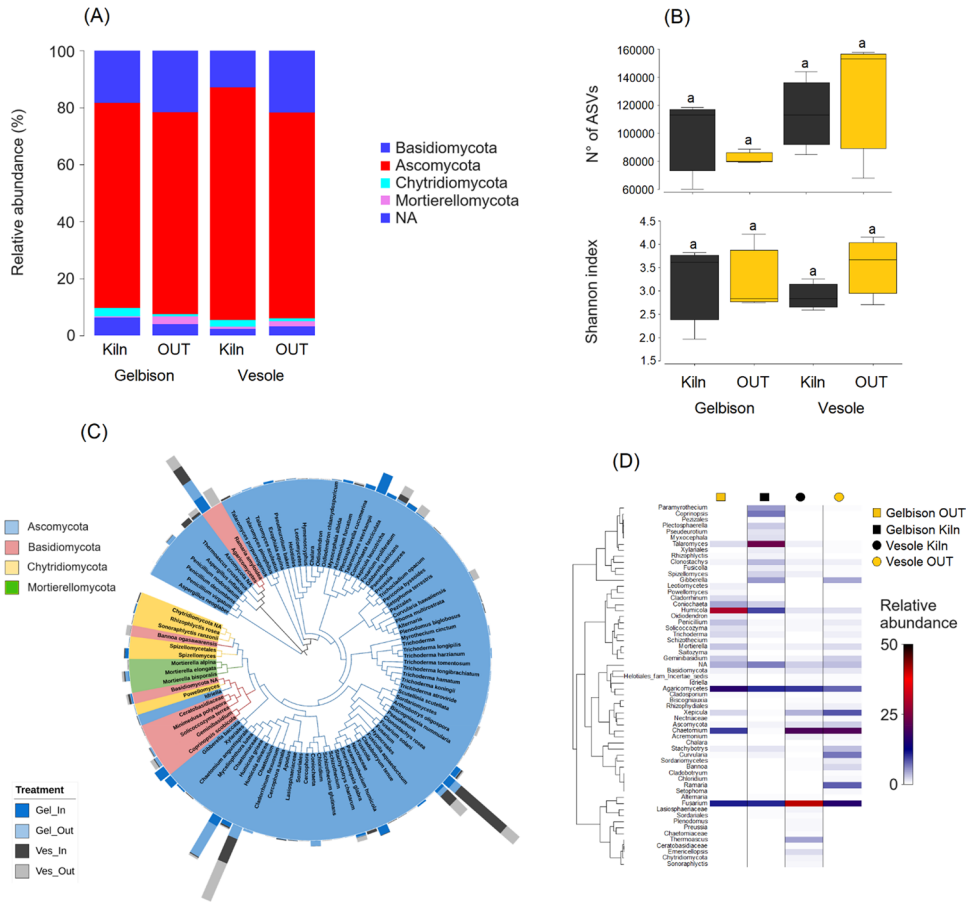

Fig. 6 **A** The relative abundance of fungal phyla inside and outside charcoal kilns on both Gelbison and Vesole mounts. **B** Box plots show the variation in the numbers of ASVs and Shannon diversity index for fungal communities inside and outside charcoal kilns on both Gelbison and Vesole mounts. Different letters indicate significant differences ($P < 0.05$) in the indices. **C** Phylogenetic tree displays the top 100 ASVs with the highest relative abundance. **D** Heatmap displays the relative abundance of the 60 most frequent Amplicon Sequence Variants (ASVs) in the fungal communities inside and outside charcoal kilns on both Gelbison and Vesole mounts. The hierarchical clustering of variables is based on Whittaker's association index

Extended error bar plots indicated statistically significant features, along with the corresponding P-values, effect sizes, and confidence intervals (Fig. 7). Taxonomic changes in the microbial community were assessed at the deepest taxonomical level. A comparison of bacterial changes inside and outside the kilns revealed a significant increase in the abundance of 18 taxa inside the Gelbison kilns, as well as a significant increase in the abundance of 4 taxa outside the kilns in Gelbison. These findings were characterized by an increase in the representation of *Anaeromyxobacter* ($P < 0.001$), *Gemmatimonadaceae* ($P < 0.001$), and *RB41* ($P = 0.034$) inside the kilns. On the other hand, soils outside soils were enriched with *Gemmatimons* ($P = 0.044$) and *WD2101* ($P = 0.045$). Concerning the fungal communities of the Gelbison, a significant increase in the abundance of 4 taxa inside the kilns and a significant increase in the abundance of 4 taxa outside the kilns were observed. Specifically, *Apiosordaria* ($P = 0.012$), *Paraboeremia* ($P = 0.016$), and *Xylariales* ($P = 0.033$) were significantly more prevalent in kilns, while *Oidiodendron* ($P = 0.026$) was more abundant outside. On the other hand, only 2 bacterial taxa were observed to exhibit a significant increase inside kilns at Vesole compared to 23 taxa outside (Fig. 8). In detail, the kiln soils were characterized by a significant increase in *TK10* ($P < 0.001$) and *Bacillaceae* ($P = 0.026$). However, soils outside showed a significant increase in *Hyphomicrobium* ($P < 0.001$), *Aetherobacter* ($P < 0.001$), *Pedobacter* ($P = 0.023$), and *SWB02* ($P = 0.045$). Nevertheless, fungal communities at Vesole were characterized by a significant increase in 4 taxa inside the kilns and a significant increase in 3 taxa outside. Specifically, *Pulvinula* ($P < 0.001$), *Sordariales* ($P < 0.001$), *Plenodomus* ($P = 0.011$), and *Chytridiomycota* ($P = 0.041$) were

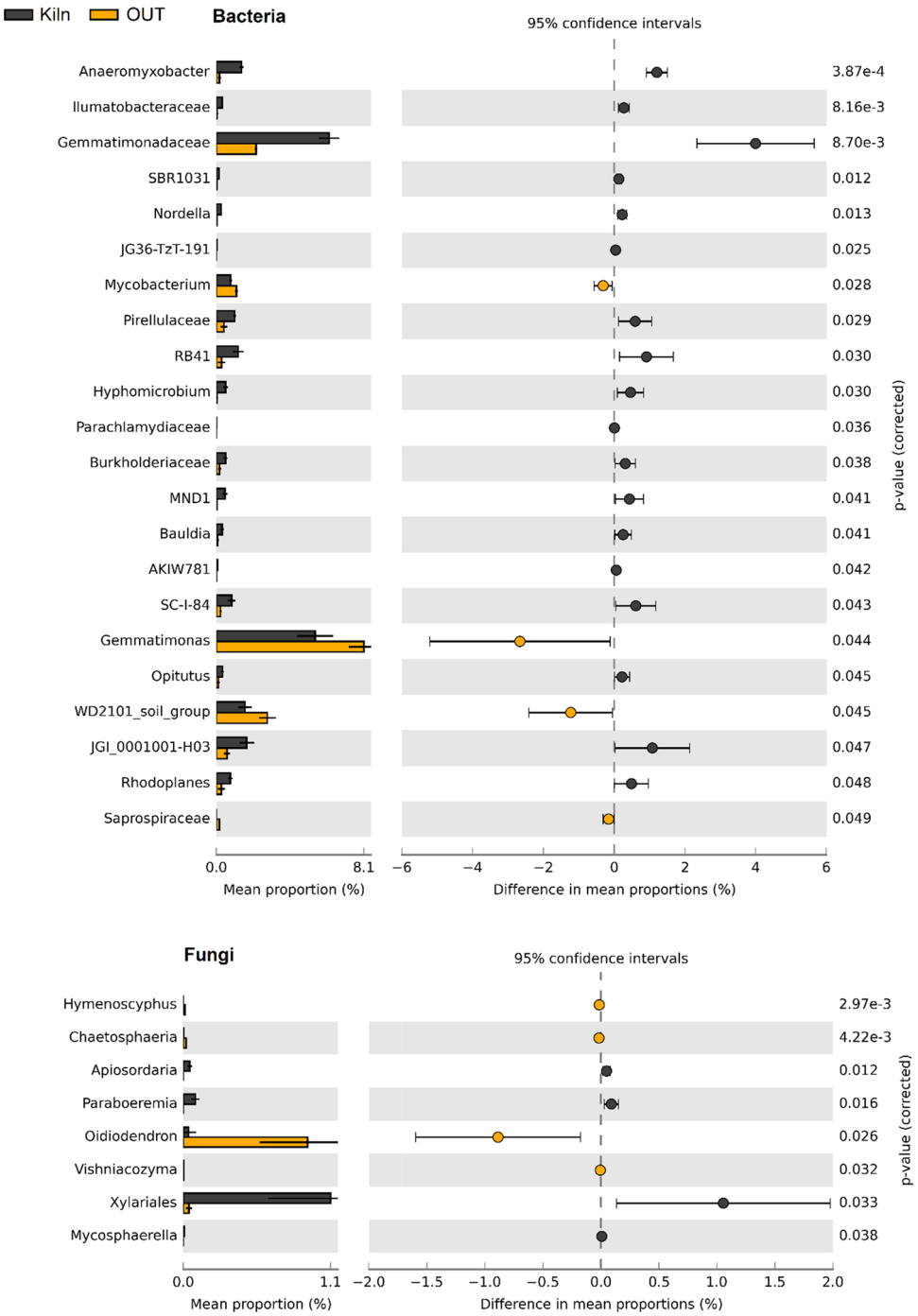

Fig. 7 Extended error bar plot identifying significant differences between mean proportions of bacterial and fungal taxa inside (black) and outside kilns (yellow) of Gelbison mount samples. Corrected p values are shown at right

significantly more abundant inside the kilns, while *Leotiomycetes* ($P<0.001$), *Auxarthron* ($P=0.012$), and *Geminibasidium* ($P=0.049$) were more abundant outside.

4 Discussion

4.1 Soil chemistry and biochar ageing

Contrary to our hypothesis, the soils of charcoal kilns do not exhibit higher pH, cation exchange capacity, and are not richer in cations i.e., Ca^{2+}, Mg^{2+}, Na^{+}, K^{+}

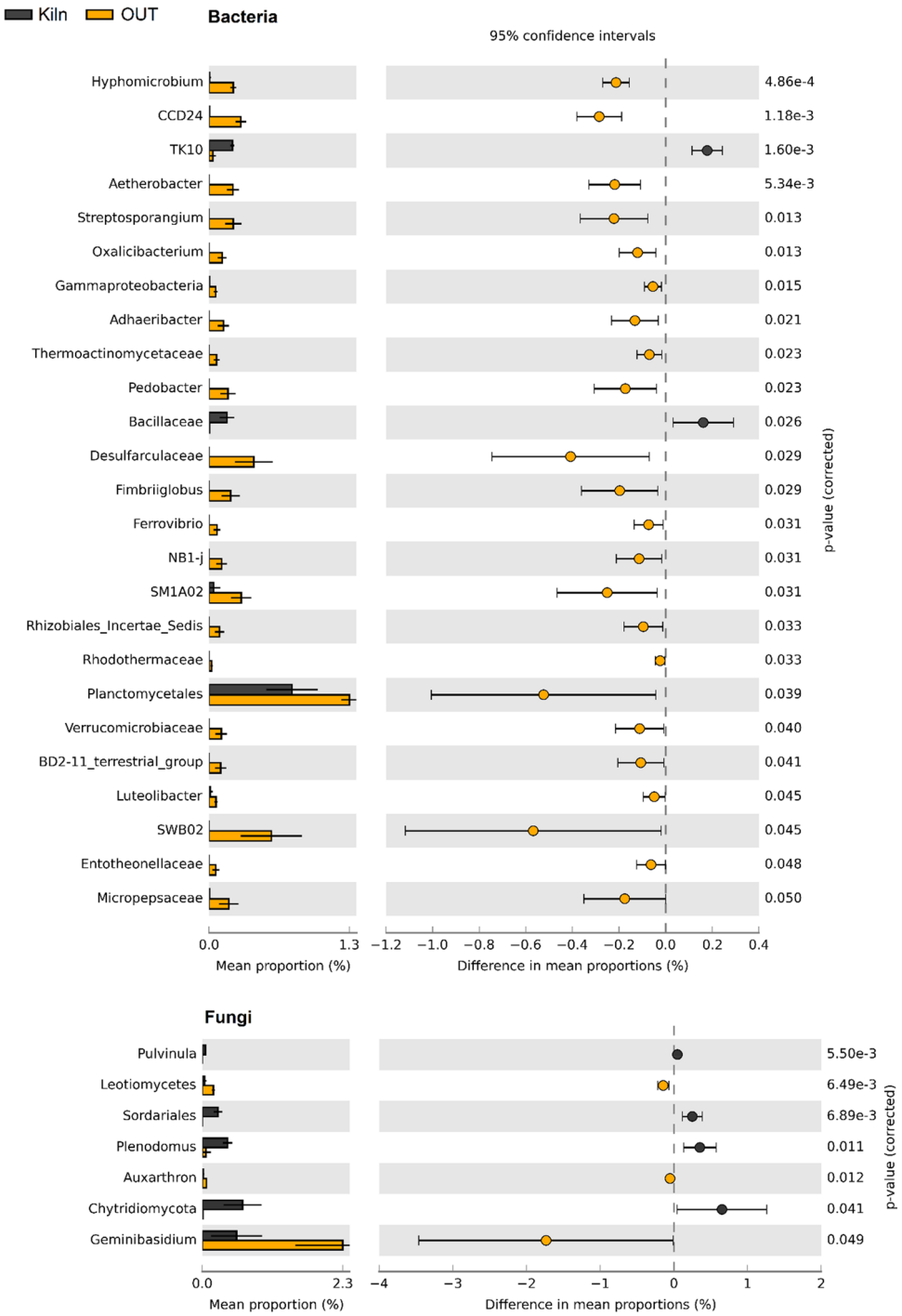

Fig. 8 Extended error bar plot identifying significant differences between mean proportions of bacterial and fungal taxa inside (black) and outside kilns (yellow) of Vesole mount samples. Corrected p values are shown at right

(Table 1). In fact, at Vesole, the soil surrounding the kiln has a higher content of main cations, organic carbon and total nitrogen. It is well known that in the phases immediately following the production of charcoal in kiln, the soil shows an increase in pH and the presence of cations (Hardy et al. 2016). However, in the subsequent decades after charcoal production, the impact tends to be mitigated by rainfall and the aging of the biochar. The rainy mountain climate (>1000 mm per year) could intensify and accelerate this phenomenon, especially considering

our estimates that suggest the charcoal pits were abandoned between 70 and 100 years ago. A reduction over time in the content of K, Mg, and P has been reported previously (Gómez-Luna et al. 2009; Ogundele et al. 2011), but in the case of Vesole, the reduction is severe compared to the external soil. Furthermore, in this case, the total organic carbon and N content is practically halved in the charcoal kiln compared to the external soil, suggesting that the intensity of the mineralization processes are involved.

In fact, high quantities of charcoal can influence enzymatic activities and overall soil respiration, as evidenced by long-term agronomic studies (Idbella et al. 2024) and comparisons in forest charcoal pits (Kučera et al. 2022). Assuming that the litter input is similar between the kiln and adjacent soil, the reduced organic carbon content could be attributed to faster mineralization in the kiln soil due to the presence of high amounts of charcoal. We must state that, in our case, in order to quantify the total carbon stock, it is necessary to add the organic carbon contained in the kiln soil to that present as coarse charcoal residues (> 2 mm) which have been estimated at 112.82 g per kg^{-1} of soil at Vesole and 157.91 g kg^{-1} at Gelbison. Indeed, charcoal kilns store significant quantities of organic carbon (Kerré et al. 2016; Fouché et al. 2023). Future studies dedicated to quantifying the carbon stock will also need to determine the density of charcoal kilns per ha of forest floor and their size to lead to an accurate estimate.

It is well known that carbon in soil is resistant to biological degradation (Lehmann and Joseph 2015), but this does not mean that carbon residues remain unchanged over time. Numerous studies have reported rapid oxidation of charcoal in short-term incubations study or by means of artificial aging approaches, reporting that BC properties were altered through the formation of oxygen-containing functional groups including carboxylic and phenolic ones (Wang et al. 2020a, b). In accordance with current knowledge, our study revealed by combining SEM–EDS spectra and FTIR that charcoal interacting with forest soil for decades undergoes substantial oxidation compared to recently produced charcoal. In fact, the O/C ratio rises considerably from 0.06 for the recent charcoal to 0.81 for Gelbison charcoal and 0.41 for Vesole charcoal, while the FTIR has shown the presence of oxygenated functional groups including phenolic, alcoholic and carboxylic. Consistently with the O/C ratio observed from SEM–EDS values, the elemental analysis showed a similar pattern with the following ratios: C/N = 93.67, for the recent charcoal, C/N = 135.07 for Vesole, and C/N = 218.33 for Gelbison samples.The study by Cheng et al. (2008) carried out in 11 historical charcoal blast furnaces distributed from Quebec to Georgia revealed substantial surface charcoal oxidation after 130 years in soils. Notably, charcoal surface oxidation increased with the mean annual temperature being significant higher in southern-located furnaces. In this context, our research based on study sites characterized by very similar climate but different bedrock allowed, for the first time, to reveal that charcoal aging process is influenced by the type of soil and basal rock. In detail, at Vesole over limestone rock the surface of the charcoal is highly enriched in Ca as well as Al and Si. On the contrary, at the Gelbison with a sedimentary and siliceous rocky substratum (flysch), Ca is practically absent on the surface of the charcoal, with abundant presence of Al and Si. The selective enrichment of the charcoal surfaces with Ca, Al, and Si as well as functional groups rich in oxygen has implications not only for the biogeochemical cycle of these elements, but also for the impact on the growth of forest plants as well as for microorganisms present in the charcoal kiln. The SEM images, in fact, also revealed the presence of a coating of probable microbial origin that covers the surface of the carbons and hides their porous structure (Hagemann et al. 2017). It is well known, in fact, that the alveolar structure of biochar can act as a colonization site for fungi and bacteria.

4.2 Soil microbiome and crop performances

In the agricultural context, it has been shown that the introduction of biochar into the soil leads to significant changes in the microbial profile in the short term (Jenkins et al. 2017; Jaiswal et al. 2018). However, the long-term consequences of these effects are not yet fully understood. A recent study conducted in a vineyard found remarkable differences in the bacterial and fungal microbiome 10 years after biochar application compared to untreated control (Idbella et al. 2024). In particular, biochar was found to contribute to an increase in the abundance of oligotrophic bacteria relative to copiotrophic bacteria. Furthermore, it led to an increase in yeasts of the genus *Basidiomycota*, while at the same time reducing the incidence of putative pathogenic fungi such as *Aspergillus*, *Fusarium* and *Phaeoacremonium*.

In our study, we investigated the long-term (> 50 years) effects of charcoal on the telluric microbiome. The differences in bacterial diversity indices could possibly be due to the different rock types present in Vesole as opposed to Gelbison. Rocks can influence soil properties and microbial communities, which in turn affects overall diversity. The limestone nature of Vesole Mountain is known to affect soil pH, which in turn affects pH-sensitive microbial communities. In addition, the presence of rock outcrops might generate microhabitats with different physical and chemical properties that form different microbial niches. On the other hand, the observed

increase in the abundance of the phyla *Gemmatimonadetes* and *Firmicutes* in the kilns could be related to their copiotrophic metabolism. *Gemmatimonadetes* and *Firmicutes* are known for their copiotrophic metabolism, a strategy that allows them to thrive in nutrient-rich environments. The increased abundance of these phyla in the kilns implies a response to the particular conditions created by the presence of charcoal, which serves as a source of carbon (Bonanomi et al. 2020). Nevertheless, *Planctomycetes* showed a strikingly high abundance outside the kilns, illustrating their oligotrophic nature. This characteristic allows them to utilize complex substrates as carbon and energy sources in nutrient-poor oligotrophic environments (Jeske et al. 2013).

As for fungal phyla, an increase in the abundance of *Basidiomycota* was observed outside the kiln sites. This remarkable increase can be attributed to the well-documented role of *Basidiomycota*, which contributes significantly to the decomposition of litter and wood in various ecosystems. The presence of diverse organic materials, including plant debris and litter, outside the kilns likely provides a rich substrate for *Basidiomycota* to thrive. Furthermore, the large number of *Basidiomycota* outside the kilns could be due to their oligotrophic nature, in contrast to the *Ascomycota* phyla. At the deepest taxonomic level, our comparison of bacterial changes inside and outside the kilns revealed a significant increase in the abundance of 18 taxa inside the Gelbison kilns, while only 4 taxa outside the kilns in Gelbison showed a similar increase. Conversely, only 2 bacterial taxa showed a significant increase inside the kilns at Vesole, compared to 23 taxa outside. These observed differences may be attributed to the specific rock types in each mount, exerting a selective influence on the flourishing and dominance of bacterial species. In particular, the kilns in both mountains have shown a significant increase in the abundance of bacterial taxa such as *Anaeromyxobacter*, *RB41*, *Gemmatimonadaceae* and *Bacillaceae*. These bacterial taxa are known as plant growth-promoting bacteria, and there is evidence that they are involved in biological nitrogen fixation in soil (Masuda et al. 2020; Wang et al. 2020a, b; Zhang et al. 2023). Similarly, the kilns have enriched several beneficial fungal taxa, including the genus *Paraboeremia*, which belongs to the dark-septate endophytic fungi, a diverse group of *Ascomycetes* that colonize plant roots. These fungi have been shown to not only promote plant growth by facilitating the uptake of carbon, nitrogen and phosphorus, but also improve the production and quantity of compounds in plants (Wu and Guo 2008; Zhang et al. 2012). They also help to protect plants from biotic and abiotic stress (Santos et al. 2017). In addition, the genus *Xylariales* has been significantly promoted by the presence of kilns. This genus has been repeatedly reported to produce biologically active volatiles that help plants defend against soil-borne pathogens (Becker and Stadler 2021).

The practical significance of our study lies in the innovative use of kiln sites for agricultural production (Coomes and Miltner 2017; Miltner and Coomes 2015), a recent practice influenced by soil properties at the kiln sites that vary depending on biochar type, site-specific soil and climatic conditions, and management practices (Glaser and Lehr 2019). In our bioassay experiments, contrary to our expectations, crop biomass was never higher in the charcoal-rich soil of kilns, and only in one case (*Solanum lycopersicum* in the Vesole soil) was it higher in the external soil. This result contradicts most agronomic studies where the addition of biochar typically increases crop productivity (Jeffery et al. 2011). It should be noted, however, that the greatest positive effects of biochar are found in tropical soils poor in nutrients and organic carbon (Jeffery et al. 2017; Schmidt et al. 2021). In this case, instead, forest soils are particularly rich in organic carbon and the main nutrients, possibly masking biochar-positive effects. However, the use of both sterile and non-sterile soil suggests that the microbiome present in the kiln has a greater beneficial effect than that of external forest soil. In fact, the trend is for a lower RSI index in both the Vesole and Gelbson soils, indicating greater growth in non-sterile soils. It is also interesting to note that the RSI values are negative or only in one case slightly positive, indicating that the forest microbiome tends to have beneficial effects on the crops tested. On the contrary, soil sterilization in the agricultural field causes an increase, often notable, in biomass, removing a microbiome with a significant component of pathogens (Bonanomi et al. 2016). In fact, sterilization with both heat and chemical means is a widespread practice in intensive agriculture (Bonanomi et al. 2021b, a). In the context of forest ecosystem dynamic, Carrari et al. (2016) reported in Central Italy that kiln was hostile microsite for the recolonization of deciduous and evergreen woody species. Our results are of limited use in this direction as the bioassay is conducted with species of agricultural interest. To understand the impact of charcoal kilns in our sites on the dynamics of forest regeneration, further studies are required, focusing on bioassays conducted with tree species present in the studied forests, such as beech, deciduous oak, and maples.

5 Conclusions

In Mediterranean forests, kiln microsites are widespread as a result of past human activities. Our present study, which combines extensive soil chemical analyses, detailed characterization of charcoal abundance and ageing, and profiling of soil microbiome by high-throughput

sequencing, has unveiled the distinctive nature of kiln microsites. Particularly noteworthy are the results on the aging of the charcoal particles, which aligns consistently with existing literature, demonstrating significant oxidation of the surfaces. Importantly, there is a different enrichment of Ca, Al, and Si influenced by the parent rock. Furthermore, the soil microbiome of charcoal kiln is enriched with some bacterial and fungal taxa that promote the growth of species of agricultural interest. Additionally, SEM images suggest the presence of an extensive organic coating on the surfaces of the carbons whose microbial taxonomic composition will be the subject of future investigations. Finally, our future studies would focus on quantifying the impact of charcoal kiln on organic carbon storage and understanding the impact on the regeneration of forest species.

Supplementary Information

The online version contains supplementary material available at https://doi.org/10.1007/s42773-024-00378-3.

Supplementary Material 1.

Acknowledgements
The authors extend their appreciation to The Researchers Supporting Project number (RSPD2024R676) King Saud University, Riyadh, Saudi Arabia.

Author contributions
All authors contributed to the study conception and design. Giuseppina Iacomino: Investigation, Resources, Visualization, Writing—Review & Editing. Mohamed Idbella: Conceptualization, Software, Validation, Formal analysis, Investigation, Data Curation, Visualization, Writing—Review & Editing. Luigi di Costanzo: Validation, Investigation, Resources, Visualization, Supervision, Writing—Review & Editing. Giandomenico Amoroso: Investigation, Resources. Emilia Allevato: Investigation, Resources. Ahmed M. Abd-ElGawad: Validation, Resources, Visualization, Writing—Review & Editing. Giuliano Bonanomi: Conceptualization, Validation, Investigation, Resources, Visualization, Supervision, Project administration, Writing—Original Draft. All authors read and approved the final manuscript.

Funding
This research did not receive any specific grant from funding agencies in the public, commercial, or not-for-profit sectors.

Availability of data and materials
The datasets used or analyzed during the current study are available from the corresponding author on reasonable request.

Declarations

Ethics approval and consent to participate
The manuscript is approved by all authors for publication. I would like to declare on behalf of my co-authors that the work described is original research that has not been published previously, and not under consideration for publication elsewhere.

Competing interests
The authors have no relevant financial or non-financial interests to disclose.

Author details
[1]Department of Agricultural Sciences, University of Naples Federico II, 80055 Portici, NA, Italy. [2]College of Agriculture and Environmental Sciences, AgroBioSciences (AgBS) program, Mohammed VI Polytechnic University (UM6P), 43150 Ben Guerir, Morocco. [3]Plant Production Department, College of Food & Agriculture Sciences, King Saud University, P.O. Box 2460, 11451 Riyadh, Saudi Arabia. [4]Task Force On Microbiome Studies, University of Naples Federico II, Naples, Italy.

Received: 1 February 2024 Revised: 6 August 2024 Accepted: 14 August 2024
Published online: 08 October 2024

References

Armas C, Ordiales R, Pugnaire FI (2004) Measuring plant interactions: a new comparative index. Ecology 85(10):2682–2686
Bayuzick S, Guarin D, Benavides J, Bonhage A, Hirsch F, Diefenbach DR, Drohan PJ (2023) Soil and geomorphic patterns within relict charcoal hearths could represent unique ecosystem niches. Geomorphology 422:108525
Becker K, Stadler M (2021) Recent progress in biodiversity research on the *Xylariales* and their secondary metabolism. J Antibiot 74:1–23
Berni Canani R, De Filippis F, Nocerino R, Laiola M, Paparo L, Calignano A, De Caro C, Coretti L, Chiariotti L, Gilbert JA (2017) Specific signatures of the gut microbiota and increased levels of butyrate in children treated with fermented cow's milk containing heat-killed *Lactobacillus paracasei* CBA L74. Appl Environ Microbiol 83:10
Bokulich NA, Mills DA (2013) Improved selection of internal transcribed spacer-specific primers enables quantitative, ultra-highthroughput profiling of fungal communities. Appl Environ Microbiol 79:2519–2526
Bolan N, Sarmah AK, Bordoloi S, Bolan S, Padhye LP, Van Zwieten L, Siddique KH (2023) Soil acidification and the liming potential of biochar. Environ Pollut 317:120632
Bonanomi G, De Filippis F, Cesarano G, La Storia A, Ercolini D, Scala F (2016) Organic farming induces changes in soil microbiota that affect agro-ecosystem functions. Soil Biol Biochem 103:327–336
Bonanomi G, De Filippis F, Zotti M, Idbella M, Cesarano G, Al-Rowaily S, Abd-ElGawad A (2020) Repeated applications of organic amendments promote beneficial microbiota, improve soil fertility and increase crop yield. Appl Soil Ecol 156:103714
Bonanomi G, Idbella M, Abd-ElGawad AM (2021a) Microbiota management for effective disease suppression: a systematic comparison between soil and mammals gut. Sustainability 13(14):7608
Bonanomi G, Zotti M, Idbella M, Mazzoleni S, Abd-ElGawad AM (2021b) Microbiota modulation of allelopathy depends on litter chemistry: mitigation or exacerbation? Sci Total Environ 776:145942
Callahan BJ, McMurdie PJ, Rosen MJ, Han AW, Johnson AJA, Holmes SP (2016) DADA2: high-resolution sample inference from illumina amplicon data. Nat Methods 13:581–583
Carrari E, Ampoorter E, Verheyen K, Coppi A, Selvi F (2016) Former charcoal platforms in Mediterranean forest areas: a hostile microhabitat for the recolonization by woody species. IFor-Biogeosci For 10(1):136
Carrari E, Ampoorter E, Bottalico F, Chirici G, Coppi A, Travaglini D, Selvi F (2017) The old charcoal kiln sites in Central Italian forest landscapes. Quatern Int 458:214–223
Chan KY, Van Zwieten L, Meszaros I, Downie A, Joseph S (2008) Using poultry litter biochars as soil amendments. Soil Res 46:437–444
Cheng CH, Lehmann J, Engelhard MH (2008) Natural oxidation of black carbon in soils: changes in molecular form and surface charge along a climosequence. Geochim Cosmochim Acta 72(6):1598–1610
Coomes OT, Miltner BC (2017) Indigenous charcoal and biochar production: potential for soil improvement under shifting cultivation systems. Land Degrad Dev 28:811–821
Cross A, Sohi SP (2013) A method for screening the relative long-term stability of biochar. Glob Change Biol Bioenergy 5:215–220
Deforce K, Boeren I, Adriaenssens S, Bastiaens J, De Keersmaeker L, Haneca K, Tys D, Vandekerkhove K (2013) Selective woodland exploitation for charcoal production. A detailed analysis of charcoal kiln remains (ca. 1300–1900 AD) from Zoersel (northern Belgium). J Archaeol Sci 40:681–689.
Deforce K, Vanmontfort B, Vandekerkhove K (2021) Early and high medieval (c. 650 AD–1250 AD) charcoal production and its impact on woodland

composition in the Northwest-European lowland: a study of charcoal pit kilns from Sterrebeek (Central Belgium). Environ Archaeol 26(2):168–178
Dey S, Purakayastha TJ, Sarkar B, Rinklebe J, Kumar S, Chakraborty R, Shivay YS (2023) Enhancing cation and anion exchange capacity of rice straw biochar by chemical modification for increased plant nutrient retention. Sci Total Environ 886:163681
Fouché J, Burgeon V, Meersmans J, Leifeld J, Cornelis JT (2023) Accumulation of century-old biochar contributes to carbon storage and stabilization in the subsoil. Geoderma 440:116717
Garbarino M, Morresi D, Meloni F, Anselmetto N, Ruffinatto F, Bocca M (2022) Legacy of wood charcoal production on subalpine forest structure and species composition. Ambio 51(12):2496–2507
Di Gennaro, A., Aronne, G., De Mascellis, R., Vingiani, S., Sarnataro, M., Abalsamo, P., & Arpaia, G. (2002). I sistemi di terre della Campania. Monografia e carta 1: 250.000, con legenda.
Glaser B (2007) Prehistorically modified soils of central Amazonia: a model for sustainable agriculture in the twenty-first century. Phil Trans Royal Soc b: Biol Sci 362(1478):187–196
Glaser B, Lehr VI (2019) Biochar effects on phosphorus availability in agricultural soils: a meta-analysis. Sci Rep 9:9338
Gómez-Luna BE, Rivera-Mosqueda MC, Dendooven L, Vázquez-Marrufo G, Olalde-Portugal V (2009) Charcoal production at kiln sites affects C and N dynamics and associated soil microorganisms in *Quercus* spp. temperate forests of central Mexico. Appl Soil Ecol 41:50–58
Hagemann N, Joseph S, Schmidt HP, Kammann CI, Harter J, Borch T, Kappler A (2017) Organic coating on biochar explains its nutrient retention and stimulation of soil fertility. Nat Commun 8(1):1089
Hardy B, Cornelis JT, Houben D, Lambert R, Dufey JE (2016) The effect of pre-industrial charcoal kilns on chemical properties of forest soil of Wallonia, Belgium. Eur J Soil Sci 67(2):206–216
Hijmans RJ, Cameron SE, Parra JL, Jones PG, Jarvis A (2005) Very high resolution interpolated climate surfaces for global land areas. Int J Climatol 25:1965–1978
Iacomino G, Sarker TC, Ippolito F, Bonanomi G, Vinale F, Staropoli A, Idbella M (2022) Biochar and compost application either alone or in combination affects vegetable yield in a volcanic Mediterranean soil. Agronomy 12(9):1996
Idbella M, Baronti S, Giagnoni L, Renella G, Becagli M, Cardelli R, Bonanomi G (2024) Long-term effects of biochar on soil chemistry, biochemistry, and microbiota: results from a 10-year field vineyard experiment. Appl Soil Ecol 195:105217
ISPRA (2023). Carta Geologica D'Italia alla scala 1:50.000.
Jaiswal AK, Elad Y, Cytryn E, Graber ER, Frenkel O (2018) Activating biochar by manipulating the bacterial and fungal microbiome through pre-conditioning. New Phytol 219(1):363–377
Jeffery S, Verheijen FGA, van der Velde M, Bastos AC (2011) A quantitative review of the effects of biochar application to soils on crop productivity using meta-analysis. Agr Ecosyst Environ 144:175–187
Jeffery S, Abalos D, Prodana M, Bastos AC, Van Groenigen JW, Hungate BA, Verheijen F (2017) Biochar boosts tropical but not temperate crop yields. Environ Res Lett 12(5):053001
Jenkins JR, Viger M, Arnold EC, Harris ZM, Ventura M, Miglietta F, Taylor G (2017) Biochar alters the soil microbiome and soil function: results of next-generation amplicon sequencing across Europe. Gcb Bioenergy 9(3):591–612
Jeske O, Jogler M, Petersen J, Sikorski J, Jogler C (2013) From genome mining to phenotypic microarrays: planctomycetes as source for novel bioactive molecules. Antonie Van Leeuwenhoek 104:551–567
Jin H (2010) Characterization of microbial life colonizing biochar and biochar-amended soils. Cornell University, Ithaca
Keeling CD (1979) The suess effect: 13Carbon-14Carbon interrelations. Environ Int 2(4–6):229–300
Keith A, Singh B, Singh BP (2011) Interactive priming of biochar and labile organic matter mineralization in a smectite-rich soil. Environ Sci Technol 45:9611–9618
Kerré B, Bravo CT, Leifeld J, Cornelissen G, Smolders E (2016) Historical soil amendment with charcoal increases sequestration of non-charcoal carbon: a comparison among methods of black carbon quantification. Eur J Soil Sci 67:324–331
Kimetu JM, Lehmann J (2010) Stability and stabilisation of biochar and green manure in soil with different organic carbon contents. Soil Res 48:577–585
Knapp H, Robin V, Kirleis W, Nelle O (2013) Woodland history in the upper Harz Mountains revealed by kiln site, soil sediment and peat charcoal analyses. Quatern Int 289:88–100
Kučera A, Holík L, Knott R, Adamec Z, Volánek J, Bajer A (2022) The soil environment of abandoned charcoal kiln platforms in a low-altitude central European forest. Forests 14(1):29
Landi, M., Piussi, P., (1988). Il lavoro nei boschi. Boscaioli e carbonai a Luco e Grezzano tra il 1930 e il 1950. Gruppo d'Erci, Istituto di Selvicoltura dell'Università degli Studi di Firenze.
Lasota J, Błońska E, Babiak T, Piaszczyk W, Stępniewska H, Jankowiak R, Boroń P, Lenart-Boroń A (2021) Effect of charcoal on the properties, enzyme activities and microbial diversity of temperate pine forest soils. Forests 12:1488
Lehmann J, Joseph S (2015) Biochar for environmental management: an introduction. In: Lehmann J, Joseph S (eds) Biochar for environmental management. Routledge, Milton Park, pp 1–13
Leite DCA, Balieiro FC, Pires CA, Madari BE, Rosado AS, Coutinho HLC, Peixoto RS (2014) Comparison of DNA extraction protocols for microbial communities from soil treated with biochar. Braz J Microbiol 45:175–183
Liu YY, Chen JW (2022) Effect of ageing on biochar properties and pollutant management. Chemosphere 292:133427
Martin M (2011) Cutadapt removes adaptor sequences from high-throughput sequencing reads. Embnetjournal 17:10–12
Masuda Y, Yamanaka H, Xu Z, Shiratori Y, Aono T, Amachi S, Senoo K, Itoh H (2020) Diazotrophic *Anaeromyxobacter* isolates from soils. Appl Environ Microbiol 86(16):e00956-e1020
Mia S, Singh B, Dijkstra FA (2017) Aged biochar affects gross nitrogen mineralization and recovery: a 15N study in two contrasting soils. Glob Change Biol Bioenergy 9:1196–1206
Miltner BC, Coomes OT (2015) Indigenous innovation incorporates biochar into swidden-fallow agroforestry systems in Amazonian Peru. Agrofor Syst 89:409–420
Nelle O (2003) Woodland history of the last 500 years revealed by anthracological studies of charcoal kiln sites in the Bavarian Forest, Germany. Phytocoenologia 33(4):667–682
Nilsson RH, Larsson KH, Taylor AFS, Bengtsson-Palme J, Jeppesen TS, Schigel D, Kennedy P, Picard K, Glöckner FO, Tedersoo L, Saar I, Kõljalg U, Abarenkov K (2019) The UNITE database for molecular identification of fungi: handling dark taxa and parallel taxonomic classifications. Nucleic Acids Res 47:D259–D264
Nocentini S, Coll L (2013) Mediterranean forests. Human use and complex adaptive systems. In: Messier C, Puettmann KJ, Coates KD (eds) Managing forests as complex adaptive systems: building resilience to the challenge of global change. Routledge, Milton Park, p 214
Novak JM, Watts DW (2013) Augmenting soil water storage using uncharred switchgrass and pyrolyzed biochars. Soil Use Manag 29(1):98–104
Ogundele AT, Eludoyin OS, Oladapo OS (2011) Assessment of impacts of charcoal production on soil properties in the derived savanna, Oyo state, Nigeria. J Soil Sci Environ Manag 2:142–146
Oleszczuk P, Rycaj M, Lehmann J, Cornelissen G (2012) Influence of activated carbon and biochar on phytotoxicity of air-dried sewage sludges to Lepidium sativum. Ecotoxicol Environ Saf 80:321–326
Pietramellara G, Ascher J, Borgogni F, Ceccherini MT, Guerri G, Nannipieri P (2009) Extracellular DNA in soil and sediment: fate and ecological relevance. Biol Fertil Soils 45:219–235
Quast C, Pruesse E, Yilmaz P, Gerken J, Schweer T, Yarza P, Peplies J, Glöckner FO (2013) The SILVA ribosomal RNA gene database project: improved data processing and web-based tools. Nucleic Acids Res 41:D590–D596
Rajapaksha AU, Chen SS, Tsang DCW et al (2016) Engineered/designer biochar for contaminant removal/immobilization from soil and water: potential and implication of biochar modification. Chemosphere 148:276–291
Santos SGD, Silva PRAD, Garcia AC, Zilli JÉ, Berbara RLL (2017) Dark septate endophyte decreases stress on rice plants. Braz J Microbiol 48:333–341
Schmidt HP, Kammann C, Hagemann N, Leifeld J, Bucheli TD, Sánchez Monedero MA, Cayuela ML (2021) Biochar in agriculture–a systematic review of 26 global meta-analyses. GCB Bioenergy 13(11):1708–1730
Schoenau JJ, Ohalloran IP (2008) Sodium bicarbonate-extractable phosphorus. Soil Sampl Methods Anal 2:89–94
Schweingruber, F. H. (1990). Anatomy of European woods. Anatomy of European woods.
Seligson KE, Negrón TG, Ciau RM, Bey GJ, Rubenstein M (2017) Search of Kilns: the forms and functions of annular structures in the Bolonchén District.

In: Rubenstein M (ed) Recent investigations in the puuc region of yucatán. Archaeopress Publishing Ltd., Gloucestershire, pp 25–38
Silverstein TP, Kirk SR, Meyer SC, Holman KL (2015) Myoglobin structure and function: a multiweek biochemistry laboratory project. Biochem Mol Biol Educ 43:181–188.
Snitker G, Moser JD, Southerlin B, Stewart C (2022) Detecting historic tar kilns and tar production sites using high-resolution, aerial LiDAR-derived digital elevation models: introducing the Tar Kiln feature detection workflow (TKFD) using open-access R and FIJI software. J Archaeol Sci Rep 41:103340
Straka TJ (2014) Historic charcoal production in the US and forest depletion: development of production parameters. Adv Hist Stud. https://doi.org/10.4236/ahs.2014.32010
Sultana N, Ikeya K, Watanabe A (2011) Partial oxidation of char to enhance potential interaction with soil. Soil Sci 176:495–501
Sumner ME, Miller WP (1996) Cation exchange capacity and exchange coefficients. Methods Soil Anal: Part 3 Chem Methods 5:1201–1229
Walkley A, Black IA (1934) An examination of the Degtjareff method for determining soil organic matter, and a proposed modification of the chromic acid titration method. Soil Sci 37(1):29–38
Wang L, O'Connor D, Rinklebe J, Ok YS, Tsang DC, Shen Z, Hou D (2020a) Biochar aging: mechanisms, physicochemical changes, assessment, and implications for field applications. Environ Sci Technol 54(23):14797–14814
Wang X, He T, Gen S, Zhang X, Wang X, Jiang D, Li C, Li C, Wang J, Zhang W, Li C (2020b) Soil properties and agricultural practices shape microbial communities in flooded and rainfed croplands. Appl Soil Ecol 147:103449
Watson RJ, Blackwell B (2000) Purification and characterization of a common soil component which inhibits the polymerase chain reaction. Can J Microbiol 46:633–642
Wiedner K, Schneeweiß J, Dippold MA, Glaser B (2015) Anthropogenic dark earth in northern Germany—the nordic analogue to terra preta de indio in Amazonia. CATENA 132:114–125
Wilkinson AJ, Britton TB (2012) Strains, planes, and EBSD in materials science. Mater Today 15(9):366–374
Wu LQ, Guo SX (2008) Interaction between an isolate of dark septate fungi and its host plant *Saussurea involucrata*. Mycorrhiza 18:79–85
Wu H, Wu H, Jiao Y, Zhang Z, Rensing C, Lin W (2022) The combination of biochar and PGPBs stimulates the differentiation in rhizosphere soil microbiome and metabolites to suppress soil-borne pathogens under consecutive monoculture regimes. GCB Bioenergy 14(1):84–103
Zhang HH, Tang M, Chen H, Wang YJ (2012) Effects of a dark-septate endophytic isolate LBF-2 on the medicinal plant *Lycium barbarum* L. J Microbiol 50:91–96
Zhang X, Li Y, Cui K, Sun Y, Zhang X, Zheng G, Zhao M, Wang B, Yang H (2023) Deciphering the turnover of bacterial groups in winter agricultural soils. Sci Total Environ 891:164672